Deciphering The Molecular Mechanism of Long Non-Coding RNA HIFA-AS1 Regulating Pancreatic Cancer Cells

He Zhang
Training Center for Clinical Skills and Medical staff，General Hospital of Northern Theater Command
Xinwei Wang
Training Center for Clinical Skills and Medical staff，General Hospital of Northern Theater Command
Yue Wu
Training Center for Clinical Skills and Medical staff，General Hospital of Northern Theater Command
Xuehua Li
Training Center for Clinical Skills and Medical staff，General Hospital of Northern Theater Command
Rui Sun
Training Center for Clinical Skills and Medical staff，General Hospital of Northern Theater Command
Jing Tian (13352459336@163.com)
Training Center for Clinical Skills and Medical staff，General Hospital of Northern Theater Command

Research Article

Keywords: pancreatic cancer, long non coding RNA, HIFA AS1 , overexpression, molecular mechanism

Posted Date: June 10th, 2021

DOI: https://doi.org/10.21203/rs.3.rs-533849/v1

Deciphering the molecular mechanism of long non-coding RNA HIFA-AS1 regulating pancreatic cancer cells

He Zhang[1, 2], Xinwei Wang[1], Yue Wu[1], Xuehua Li[1], Rui Sun[1], Jing Tian[1*]

[1]Training Center for Clinical Skills and Medical staff，General Hospital of Northern Theater Command, No.83, Wenhua Road, Shenhe District, Shenyang, 110016, China;

[2]Laboratory Animal Center, General Hospital of Northern Theater Command, No.83, Wenhua Road, Shenhe District, Shenyang, 110016, China.

* Corresponding author: Jing Tian; e-mail: 13352459336@163.com.

Abstract

Background：*HIFA-AS1*, an antisense transcript of *HIF1α* gene, is a 652-bp long non-coding RNA (lncRNA) which globally expressed in multiple tissues of animals. Recent evidence indicated that the *HIFA-AS1* was involved in tumorigenesis of several types of cancer, but there were no reports on pancreatic cancer (PC).

Results: In order to investigate whether the *HIFA-AS1* could mediate the PC or not, it was overexpressed in a PC cell line (PANC-1), and a series of experiments including cell viability detection, flow cytometry, transwell migration, clone formation and wound healing were performed. Functionally, the results indicated that overexpression (OE) of *HIFA-AS1* could inhibit proliferation and shift, and promote apoptosis of PC cells. Moreover, to explore underlying molecular mechanism of anti-tumorigenic actions of *HIFA-AS1* in PC cells, the iTRAQ (isobaric tags for relative and absolute quantification) quantitative proteomics analysis was implemented and the results indicated that OE of *HIFA-AS1* globally affected the expression levels of multiple protein associated with metabolism of cancer. Moreover, the network analysis revealed that the most of these differentially expressed proteins (DEPs) were integrated, and severed essential roles in regulatory function.

Conclusions: In summary, *HIFA-AS1* may exhibit a potential therapeutic effect on PC, and our study provided useful information in this filed.

Keywords: pancreatic cancer, long non-coding RNA, *HIFA-AS1*, overexpression, molecular mechanism

Introduction

Pancreatic cancer (PC) remains one of the most common causes of cancer-related mortality [1] at the seventh in humans worldwide [2], with 5-year overall survival rate of less than 5% [3]. In most cases, PC develops with usually clinically silent at the early stage, but the variable symptoms, local invasiveness, or metastases only develop at an advanced stage [4]. Nowadays, the therapeutic efficacy of PC treatment is still very limited, and far from satisfactory [5, 6]. Hence, in order to enhance the cure rate of PC, it is necessary to investigate the molecular mechanisms, which would provide new opportunities to improve effective therapeutic strategies against PC.

Long non-coding RNAs (lncRNAs), a kind of non-coding RNAs transcripts, comprises longer than 200 bp without protein-coding potential [7-9]. Current studies have showed that lncRNAs could mediate gene expression via chromosome remodeling, transcription and post-transcriptional processes [10]. As so far, increasing evidences demonstrate that lncRNAs play an important role in regulating vital molecular mechanism [11] and biological functions of the cells [12, 13], such as proliferation, migration, invasion, cell cycle and apoptosis [14-16]. Without a doubt, various expression of lncRNAs could contribute to tumor development and progression [17], but its regulatory mechanism had not been completely investigated.

HIFA-AS1 is an antisense transcript of *HIF1α* [18], and accumulating evidence has revealed that it plays a key role in proliferation and apoptosis of vascular smooth muscle cells [19-21], and human hepatic stellate cells [22]. Furthermore, it promotes tumor necrosis factor-α-induced apoptosis [23], thereby affecting the occurrence and

development of thoracic aortic aneurysm [24]. *HIF1A-AS1* can regulate starvation-induced hepatocellular carcinoma cell apoptosis, promoting hepatocellular carcinoma (HCC) cell progression [25]. Therefore, *HIFA-AS1* has the capacities to affect the occurrence and development of multiple types of cancer, but there is no report on the molecular regulation mechanism of *HIFA-AS1* in PC.

In the current study, to explore whether *HIFA-AS1* could regulate PC or not, we constructed overexpression (OE) plasmids containing *HIFA-AS1*, and transferred them to a PC cell line. Subsequently, a series of experiments, including cell viability detection, flow cytometry, transwell migration, clone formation and would healing were conducted. And the experimental results showed that OE of *HIFA-AS1* could inhibit proliferation and metastasis, and promote apoptosis of PC cells, comparing with the normal control (NC) cells. In order to further explore the molecular mechanism of *HIFA-AS1* regulating PC cells, we collected cell samples from OE and NC groups for iTRAQ (isobaric tags for relative and absolute quantification) proteomics experiments. Here we report the results.

Materials and methods

Cell culture

The human pancreatic cancer cell line (PANC-1) was provided by Procell (Wuhan, China) and cultured in monolayers in Dulbecco's modified Eagle's medium (DMEM) (Invitrogen, Carlsbad, USA). All media were supplemented with 10% fetal bovine serum (Hyclone UT, USA) in the presence of 100 U/ml penicillin and 50 μg/m streptomycin (Beyotime, Shanghai, China) with humidified atmosphere of 5% CO_2 and 95% air at 37 °C.

Plasmid construction, Lentivirus package and transfection

HIFA-AS1 was cloned into the pcDNA3.1(+) vector using the restriction sites for *Kpn*I (GGTACC) and *Xho*I (CTCGAG), and this 652 bp insert was verified by sequencing. Two μg of plasmids containing *HIF1A-AS1* were mixed with the lentivirus packaging plasmids pMDLg-pRRE, pMD2.G, and pRSV-Rev according to the previous standard protocol [26]. Subsequently, PANC-1 cells were infected with 20 multiplicity of infection (MOI) lentivirus for 24 h and incubated in fresh medium. The cells were washed with fresh complete media after 24 h and the efficiency OE of *HIF1A-AS1* was verified by quantitative RT-PCR (qRT-PCR).

RNA extraction and qRT-PCR

Total RNA was extracted from the cells using TRIzol reagent (Ambion, Austin, USA) and further purified with two phenol-chloroform treatments, then treated with RQ1 DNase (Promega, Madison, USA) to digest DNA. The quality and quantity of the purified RNAs were determined using a Nano Photometer spectrometer with the absorbance at 260 nm/280 nm and next were verified by 1.2% agarose gel electrophoresis. The cDNA was synthesized with random primers with the High-capacity cDNA Reverse-Transcription Kit (Takara, Dalian , China), and real time PCR was implemented for detecting gene expressions using the designed primers in Table 1 with SYBR Green I dye (Qiagen, Hilden, Germany). The PCR conditions were as follows: pre-denaturation at 95 °C for 1 min, 40 cycles of denaturing at 95 °C for 15 s, annealing at 60 °C for 30 s and elongation at 72 °C for 40 s. The relative expression of genes was analyzed by the $2^{-\triangle\triangle CT}$ method with the *Actin* as an internal control [27].

Cell viability detection

The viability of PANC-1 cell was evaluated using the CCK-8 assay (Solarbio, Peking,

China) according to the instructions of the manufacturer. The cells were slightly seeded into the 96-well plates with 100 μl suspension per well overnight. At 0, 24, 48 and 72 h, 10 μl of CCK-8 solution was added to each well, and then the plates were incubated for 0.5 h. At last, absorbance was measured at 450 nm by microplate reader (Bio-Rad, Hercules, USA).

Flow cytometric detection

The apoptosis of the PANC-1 cells were determined by flow cytometry with Annexin V-conjugated FITC Apoptosis detection kit (BD, Franklin Lakes, USA). After infection for 24 h, cells were harvested and washed twice with PBS, then re-suspended in 5μl FITC-conjugated anti-Annexin V antibody and in 500 μl binding buffer with 5μl Propidium iodide (PI). Apoptosis was measured with a FACS calibur flow cytometer MoFLO XDP (Beckman, Hercules, USA).

Transwell invasion

For the transwell assay, the properties of migration of cells were evaluated by using 24-well transwell plates (Corning, NY, USA). About 1×10^4 cells per well were seeded into the upper chamber with serum free medium in triplicate. Medium containing 10% FBS (300 μl) was added to the DMEM of 5% CO_2 and 95% air at 37°C. After incubation for 24 h, the medium were removed, and cells were fixed with 4% paraformaldehyde for 15 min, stained with 0.1% crystal violet for 20 min, and counted from five randomly chosen fields for each well by stereo microscope (Leica, Wetzlar, Germany).

Wound Healing Assay

After 12 h of the transfected cells were seeded in 6-well plates, confluent monolayers in each well were washed with PBS and created using a 200 μl sterile pipette tip to

generate a wound. Wound healing was evaluated and photographed images were taken by 200 magnification a Zeiss microscope (Leica, Wetzlar, Germany) from each well at 0, 24, and 48 h post-injury time points after the wound was made.

Cell clone formation assay

PANC-1 cells were plated into 6-well plates (800 cells per well) and cultured for 10–14 days, then were digested at the logarithmic phase to make a single-cell suspension using culture medium. Cell were stained with 0.4% crystal violet (Bio Basic Inc., Markham, Canada). Finally, the number of colonies was calculated under an inverted microscope (Leica, Wetzlar, Germany).

Western Blotting Analysis

PANC-1 cells were collected and the homogenates were centrifuged for 30 min at 4 °C, 12,000 rpm with cell lysis buffer. Then the protein extracts were separated on 10% SDS-PAGE and transferred to polyvinylidene difluoride (PVDF) membranes. Membranes were incubated at room temperature for 1 h in a 5% skim milk TBST blocking solution and incubated with agitation at 4 °C overnight with specific primary antibodies anti-GAPDH (Beyotime, Shanghai, China), anti-Bax (Cell signaling technology, Beverly, MA, USA), anti-P53 (Szybio, Wuhan, China), anti-Caspase 3 (Cell Signaling Technology), and anti-PARP-1 (Cell Signaling Technology). Next, membranes also were incubated with secondary antibodies conjugated by horseradish peroxidase (HRP) (Zhong san jinqiao, Beijing, China) for 50 min at room temperature. At last, protein bands were determined using the Western blotting detection system (GE Healthcare, Amersham, UK).

iTRAQ quantitative proteomics analysis

For protein extraction from the cells (5×10^6), the lysis buffer (7M Urea/2M Thiourea/4% SDS/40 mM Tris-HCl, pH 8.5) that contains 1 mM phenylmethanesulfonyl fluoride (PMSF) and 2 mM ethylenediaminetetraacetic acid (final concentration) was added to the sample, mixed and incubated in ice for 5 min. Subsequently, DL-Dithiothreitol (DTT) was added to a final concentration of 10 mM. The lysate was sonicated on ice for 20 min, then centrifuged at 4 °C, 13,000 g for 25 min. The supernatant was mixed with four volumes of precooled acetone and kept at -20 °C overnight. After centrifugation, the protein pellets were air-dried and re-dissolved in 8M urea/100mM triethylamine borane (TEAB) (pH=8.0). Protein samples were reduced with 10 mM DTT at 56 °C for 35 min and alkylated with 50 mM iodoacetamide (IAM) in the dark at room temperature for 30 min. The supernatant was transferred to a new centrifuge tube, and the protein precipitation was performed by acetone precipitation. The protein pellet was re-dissolved by adding 8 M urea/100 mM TEAB (pH=8.0) solution, and DTT was added to a final concentration for 10 mM, with reduction reaction at 56 °C for 25 min. Subsequently, IAM was added to a final concentration for 55 mM, and the alkylation reaction was carried out at room temperature for 40 min in the dark. The protein concentration was assessed by the Bradford method.

The 100 μg protein were trypsin digested with trypsin each sample. After diluting the protein solution 5 times with 100 mM TEAB, trypsin were added by a mass ratio of 1:50 (trypsin: protein) overnight at 37 °C. The peptides were desalted with C_{18} column after enzymolysis, and the desalted peptides were vacuum freeze-dried.

The mass spectrometry data was collected and analyzed using the Eksigent nanoLC

system (SCIEX, USA) coupled to the TripleTOF 5600+ mass spectrometers. Samples were iTRAQ labeled as follows: NC-1, X1; NC-2, X2; NC-3, X3; OE-1, X4; OE2, X5; and OE-3, X6. And all of the labeled samples were mixed with equal amounts. Next, the polypeptide solution was added to analytical ChromXP C_{18} column (Bonna-Agela Technologies Inc., Wilmington, DE) (5 μm, 100 Å, 4.6×250 mm), and eluted at 300 nl/min on a C_{18} analytical column (3 μm, 75 μm× 150 mm) over 90 min gradient. The two mobile phases were used both buffer A (2% acetonitrile / 0.1% formic acid / 98% H_2O) and buffer B (98% acetonitrile / 0.1% formic acid / 2% H_2O). For Information Dependent Acquisition (IDA), the first-order mass spectrum was scanned with an ion accumulation for 250 ms, at the same time the secondary mass spectrum of 30 product ion scans were collected with 50 ms. The MS1 spectrum was acquired in the range 350-1500 m/z, and the MS2 spectrum was acquired in the range 100-1500 m/z. Precursor ions were set from reselection for 15 s.

The original MS/MS file data were analyzed using ProteinPilot Software v4.5 (AB Sciex, Shanghai, China). For protein identification, the Paragon algorithm, which was integrated into ProteinPilot, was used against the UniProt/SwissProt database for database searching. The parameters were set as follows: the instrument was TripleTOF 5600+, iTRAQ quantification, and cysteine modified with IAM, and biological modifications were selected as ID focus, trypsin digestion, quantitate, bias correction, and background correction was used for protein quantification and normalization. For calculation of the false discovery rate (FDR), an automatic decoy database search strategy was used to estimate FDR using the proteomics system performance evaluation pipeline software (PSPEP, integrated into the ProteinPilot Software). Unique peptides were used for iTRAQ labeling quantification, and peptides with global FDR values from fit less than 1% were considered for further analysis. Within each iTRAQ run,

differentially expressed proteins (DEPs) were determined based on the ratios of differently labeled proteins and p values provided by ProteinPilot, the p values were generated by ProteinPilot using the peptides used to quantify the respective protein. For the determination of DEPs, fold changes (FC) were calculated as the average comparison pairs among biological replicates. Proteins with FC larger than 1.2 and a $p < 0.05$ were considered to be changes that are significantly different.

Bioinformatics and annotations

The biological and functional properties of all the identified proteins were analyzed by matching to NCBInr (http://www.ncbi.nlm.nih.gov/) and Swiss-Prot/UniProt (http://www.uniprot.org/) databases, and were mapped with Gene Ontology (GO, http://www.geneontology.org/) and the Cluster of Orthologous Groups of proteins (COGs, http://www.ncbi.nlm.nih.gov/COG/) databases. The pathway enrichment analysis and metabolic pathways about the identified proteins were annotated by Kyoto Encyclopedia of Genes and Genomes (KEGG) mapping (http://www.genome.jp/kegg/). STRING v10.1 (http://string-db.org/) was applied to explore and analyze the protein-protein interaction (PPI) information of DEPs to evaluate the interactive associations. The PPI network was constructed and visualized using Cytoscape software (version 3.5.1; www.cytoscape.org).

Statistical analyses

All data analysis was performed using the SPSS16.0 statistical software as the mean ± standard deviation. Statistically significant differences comparison between two groups means were analyzed by Student's t-test. P value <0.05 was considered to be statistically significant.

Data availability statement

The datasets generated and/or analysed during the current study are available in the Pr otemXchange repository(Accession No: IPX0003153000). For the interview, the data sets could also be obtained from a web link: https://www.iprox.org/page/PSV023.html;?url=1622727859237GpMj, with a code: **E 5xT**.

Results

HIFA-AS1 regulates the apoptosis and proliferation of PC cells

To investigate the role of *HIFA-AS1* in the PC cells, an OE vector containing the *HIFA-AS1* was transfected into PANC-1 cells. The qRT-PCR experiment was applied to measure the efficiency of OE , and the results showed that expression levels of *HIFA-AS1* in OE cells was about 10000-fold more as compared with the normal control (NC) cells (**Fig. 1A**), demonstrating a successful establishment of human PC cells with OE of *HIFA-AS1*.

To explore whether the *HIF-AS1* regulate the proliferation of PC cells or not, the experiments including CCK-8, were conducted for PANC-1 cells from OE and NC groups. The results indicated that viability cells with *HIF-AS1* OE was declined significantly, during varying time periods (0, 24, 48 and 72h) ($P<0.001$) **(Fig. 1B and C**).

Furthermore, flow cytometry was used to determine whether *HIF-AS1* could affect apoptosis of PANC-1 cells or not. It (**Fig. 1D and E**) displayed that the OE of *HIF1A-AS1* significantly promoted apoptosis of PC cells, and the number of apoptotic cells

obviously increased about 50% compared with the NC group (**Fig. 1D**). The above results indicated that *HIF1A-AS1* had the capacities to regulate proliferation and apoptosis of the PC cells. Further, western blot analysis reported that the expression levels of Cleaved caspase-3, Bax, P53, and PARP-1A protein were higher in OE group (**Fig. 1F**), thereby inducing apoptosis in pancreatic cancer.

HIFA-AS1 regulates the migration of PC cells

To further explore the role of *HIF1A-AS1* in regulating metastasis of PANC-1 cells, the transwell migration assays were performed. It showed that the migration ability of cells from OE group was reduced about 50% ($P<0.001$) (**Fig. 2A and B**). In terms of cell clone, the clones formed in NC had a greater cell number about 45% compared with OE (**Fig. 2C and D**). Cell migration was detected using Wound-healing assay in PANC-1 cells. The results from invasion assay showed that OE of *HIF-AS1* promoted cell invasion after transfection for 24 and 48 hours (**Fig. 2E**). And the difference of the wound width after 24 hours of transfection is the most significant compared with the comparison, which exceeds the control by about 20% (**Fig. 2F**), suggesting a functional role for *HIF1A-AS1* in inhibiting metastasis of the PC cells.

The summary of iTRAQ proteomics analysis

To explore the molecular mechanism of *HIFA-AS1* mediating the proliferation, apoptosis and shift of PANC-1 cells, an iTRAQ was applied to uncover altered protein expressions and signaling pathways.

In total, the quality of the data obtained from the iTRAQ was analyzed using parameters

such as coefficient of variation about repeatability, distribution of unique peptide, peptide length, and distribution of coverage (**Table 2**). First of all, for the repeatability, there is a little difference concentration of CV data between NC and OE groups, and the cumulative percentages of CV were 7.81 % and 7.29 % respectively, indicating that the PANC-1 samples in each group are more reproducible (**Fig. 3A**).

In accordance with unique peptide determined as the peptide identified only for one protein, the presence of the corresponding protein can be uniquely determined. Then for the distribution of unique peptide number, the two-coordinate distribution map showed the number of unique peptides contained in all the proteins identified in this assay. For example, when the x-axis, left y-axis and right y-axis are 2, 646 and 26.25 respectively, it means that there are 646 proteins with 2 as the unique number of peptides, which account for 26.25% of the total number of proteins obtained **(Fig. 3B)**.

Subsequently, the length of the identified peptides was analyzed. The average length of the polypeptide was 11.56 and within a reasonable range. Moreover, the length of the identified peptides was mainly concentrated between 7 and 15, and 9 was the maximum number **(Fig. 3C)**. In addition, the protein identification coverage could reflect the overall accuracy of the identification results indirectly. The different colored pie represented the percentage of proteins with different identification coverage ranges. It showed that 37.21% proteins were with the peptide coverage less than 10%, and 39.51% proteins had more than or equal to 20% of the peptide coverage, with the average protein identification coverage being 19.53% **(Fig. 3D)**.

A total of 4872 proteins were identified in all samples, and 4738, 2475 and 2539 ones were annotated successfully by GO, COG and KEGG, respectively **(Fig. 3E)**. Particularly, the GO enrichment for the 4738 annotated proteins was carried out, including cellular localization (CC) (Data not shown), molecular functions (MF) (Data not shown) and biological processes (BP). The BP classification showed that most of these proteins were enriched in cellular process (13.04%), metabolic process (11.26%), biological regulation (8.55%), regulation of biological process (8.13%), cellular component organization or biogenesis (7.00%) and so on (**Fig. 3F**).

Exploration of DEPs and functional analysis

On basis of the relative quantitative results, 338 DEPs were found in OE *VS* NC according to FC and p value (FC $\geq$ 1.2 or $\leq$ 0.83, p $\leq$ 0.05), and the up-regulated and down-regulated ones were 183 (**Table 3**) and 155 (**Table 4**), respectively. The protein abundance distribution graph, and the volcano plot showed the proportion of DEPs in the total identified proteins (**Fig. 4A and 4B**). A hierarchical clustering analysis of DEPs was also performed (**Fig. 4C**).

In addition, KEGG enrichment for DEPs was implemented. It can be seen from the pie chart that the top 10 pathways were different among all up-regulated and down-regulated proteins. KEGG pathway enrichment was also variable across the up-regulated proteins group and down-regulated proteins group. The enriched pathways for up-regulated proteins, include “RNA transport” (ID: ko03013), “Metabolic pathways” (ID: ko01100), “Ribosome” (ID: ko03010), “Spliceosome” (ID: ko03040), “Microbial metabolism in diverse environments” (ID: ko01120), “Pathogenic

Escherichia coli infection" (ko05130), "Protein processing in endoplasmic reticulum" (ko04141), "Purine metabolism" (ko00230), "Glycolysis/ Gluconeogenesis" (ko00010), "Focal adhesion" (ko04510) and so on.

Furthermore, down-regulated proteins were primary enriched in some pathways, including "Metabolic pathways" (ID: ko01100), "Protein processing in endoplasmic reticulum" (ID: ko04141), "Pathways in cancer" (ID: ko05200), "Arrhythmogenic right ventricular cardiomyopathy" (ID: ko05412), "Microbial metabolism in diverse environments" (ID: ko01120) and "Regulation of actin cytoskeleton" (ko04810), "Tight junction" (ko04530), "Hypertrophic cardiomyopathy (HCM)" (ko05410), "Peroxisome" (ko04146), "Dilated cardiomyopathy" (ko05414) and so on (**Fig. 4D**).

According to these results indicate that the inhibitory effects of *HIF1A-AS1* on the proliferation, apoptosis and migration of PANC-1 cells may be related to its capability to regulate protein interactions, catalytic activity and enzyme regulator activity. The top 10 pathway metabolic function types were different in all up-regulated and down-regulated differential proteins by KEGG. Four types were same containing metabolic pathway, regulation of actin cytoskeleton, microbial metabolism in diverse environment, protein processing in endoplasmic reticulum. Pathway analysis revealed that "Metabolic pathways" at the second of up-regulated genes and at the first in down-regulated genes in the enrichment results. Moreover, OE of *HIF1A-AS1* may exhibit anticancer effects by regulating the pathways associated with metabolism of cancer. Therefore these results suggested that *HIF1A-AS1* might affect RNA polymerase to

control the transcription of downstream tumor-associated genes as to antagonize the proliferation, apoptosis and migration of PC cells.

Construction of DEPs Protein-protein interaction (PPI) network

PPI network of common DEPs was constructed by the STRING online database and Cytoscape software to analyze the interactions of DEPs because the String database could identify interactions between known proteins and predictive proteins (**Fig. 5**). A total of 338 DEPs (155 down-regulated and 183 up-regulated) were filtered into the DEPs PPI network complex. The wonderful network suggested that these DEPs might work together to regulate apoptosis, proliferation and invasion of PC cells. These proteins are expected to become targets for the treatment of PC.

Expression Validation by qRT-PCR

To confirm the veracity and reliability of the proteomic assays, the expression levels of five candidate proteins were measured by qRT-qPCR, including *MX1* (Interferon-induced GTP-binding protein Mx1), *IFIH1* (Interferon-induced helicase C domain-containing protein 1), *IFIT1* (Interferon-induced protein with tetratricopeptide repeats 1), *ISG15* (Ubiquitin-like protein ISG15), *P4HB* (Protein disulfide-isomerase), *SOD2* (Superoxide dismutase [Mn], mitochondrial) (**Fig. 6**). Some specific primers were designed for these candidate (**Table 1**). *MX1*, *IFIH1*, *IFIT1* and *ISG15* mRNAs showed more than 2-fold down-regulation as compared to NC (**Fig 6A, B, C and E**) and *P4HB* more than 0.5- fold down-regulation (**Fig. 6D**). In addition, *SOD2* showed 2 fold up-regulation (**Fig. 6F**). In short, above data supported that the results of the proteome was

of credibility.

Discussion

PC remains one of the deadliest cancer types and worlds' most aggressive malignancies [28]. Accumulating reports have reported that the potential of lncRNAs as diagnostic or prognostic biomarkers ubiquitously dysregulated and have crucial regulatory roles in tumor cells, including PC [29]. However, the regulatory mechanisms of multiple lncRNAs are elusive in many kinds of cancers such as thoracic aortic aneurysm and HCC. Herein, we first aimed to explore the molecular mechanisim of *HIF1A-AS1* regulating PC.

In the present study, we investigated the biological function of *HIF1A-AS1* on proliferation, apoptosis, and metastasis of PC cells. Consistently, it was found that *HIF1A-AS1* was a suppressor of cell growth and progression in PC. Firstly, up-regulation of *HIF1A-AS1* inhibited cell growth and promoted apoptosis in PANC-1 cancer cells. Moreover, *HIF1A-AS1* inhibited cell migration. Actually, the function of *HIF1A-AS1* in other tumors has been reported. For instance, higher expression of *HIF1A-AS1*, a novel diagnostic predictor, could be clinically functioned as a potential biomarker in colorectal carcinoma [30]. Besides, the levels of *HIF1A-AS1* were significantly increased in tumor tissues or serum from non-small cell lung cancer patients [31]. Above reports researched with clinical samples, but may be the opposite with this study using PC cells. Therefore, this study indicated *HIF1A-AS1* as an important role for a novel mechanism in the PC modulated progress, could develop as a potential therapeutic target or biomarker for PC prevention and control.

The quantitative proteomics analysis revealed that the expression levels of *SOD2* was up-regulated. Previous studies have revealed that *SOD2* has both tumor suppressive and promoting functions, which are primarily related to its role as a mitochondrial superoxide scavenger and H_2O_2 regulator [32]. *SOD2* is role as both a tumor suppressor in early tumorigenesis and as a tumor promoter during metastatic progression [33]. Therefore, *HIF1A-AS1* could regulate *SOD2* to inhibit the metabolic developmental process in PC. In addition, *Mx1* expression was inversely correlated with prostate cancer [34]. However, in this study the expression levels of *MX1* was positive correlation with PC. *MX1* [35], the members of IFN-stimulated genes [36], *HIF1A-AS1* could regulate *MX1* of type I interferon-mediated signaling pathway to restrain PC. According to previous reports, *IFIT1* [37], OE of *IFIT1* involved in a variety of biological processes, such as cell proliferation, migration and tumor growth [38, 39]. In this review, we hypothesize that *HIF1A-AS1* could inhibit *IFIT1* to regulate the cell proliferation, migration to restrain PC to some extents. *IFIH1*, may play an important role in enhancing natural killer cell function and may be involved in growth inhibition and apoptosis in several tumor cell lines [40, 41]. In a word, the involvement of *IFIH1* in the growth inhibition and apoptosis of PANC-1 cancer cells was regulated by *HIF1A-AS1*. *ISG15*, induce natural killer cell proliferation, act as a chemotactic factor for neutrophils and act as an IFN-gamma-inducing cytokine lays a substantial role in the antiviral state induced by IFN [42, 43]. Further, we showed that inhibition of PC by *HIF1A-AS1* and *ISG15* is sufficiently. In line with these studies, the present findings demonstrated that *HIF1A-AS1* might regulate some tumorigenesis of PANC-1 cancer

cells via targeting interferon-mediated signaling pathway, ubiquitin system and H_2O_2 regulator all closely related to metabolic pathways in cancer. In addition, tumor-suppressive role *HIF1A-AS1* positively regulated the expression of *SOD2*, and negatively regulated the five gene expression related to metabolic regulation to suppress PC growth and progression.

In summary, these findings demonstrated that *HIF1A-AS1* could inhibit cell growth and progression of PANC-1 cells. In the future studies about diagnostic specificity and sensitivity of *HIF1A-AS1*, may be used as a potential biomarker and guidance for early diagnosis of PC. Although clinical applications need to be further explored, these results further provided insight into the molecular mechanisms associated with the tumorigenesis and scientific experimental basis for the treatment of PC.

Declarations

Ethics approval and consent to participate

Not applicable.

Consent for publication

Not applicable.

Availability of data and materials

The datasets generated and/or analysed during the current study are available in the Pr otemXchange repository(Accession No: IPX0003153000). For the interview, the data sets could also be obtained from a web link: https://www.iprox.org/page/PSV023.html;?url=1622727859237GpMj, with a code: **E 5xT**.

Competing interests

The authors declare that they have no competing interests.

Funding

Supported by Natural Science Funding of Liaoning Province (#2019-ms-350) and SYDW [2018]09 Laboratory Animals Project Funding of Military.

Author Contribution

He Zhang, Rui Sun and Jing Tian designed and managed the project. He Zhang, Xinwei Wang and Yue Wu drafted the manuscript. Xuehua Li, Rui Sun and Jing Tian participated in sample collection and manuscript revision. All authors read and approved the final manuscript.

Acknowledgement

Supported by Natural Science Funding of Liaoning Province (#2019-ms-350) and SYDW [2018]09 Laboratory Animals Project Funding of Military.

Figure 1. Overexpression (OE) of *HIFA-AS1* affects the proliferation, apoptosis of the pancreatic cancer (PC) cells (Pan-1). (A) Real-time PCR showed that the levels of *HIF1A-AS1* was significantly increased in the cells from OE group compared with normal control (NC). (B) & (C) OE of *HIF1A-AS1* reduces significantly the viability of PC cells at 24, 48, and 72 h. (D) OE of *HIF1A-AS1* promotes significantly apoptosis of PC cells assessment of cellular apoptosis using Annexin V‐fluorescein isothiocyanate staining coupled with flow cytometry. (E) Total percentage of apoptotic PANC-1 cells in each group are summarized with data presented as the mean ± SD of three independent experiments. (F) Western blotting reveal Cleaved caspase-3, Bax, P53, and PARP-1A protein expression in PANC-1 cells. ***P<0.001

Figure 2. Overexpression (OE) of *HIF1A-AS1* regulates metastasis of the pancreatic cancer (PC) cells (Pan-1). (A) & (B) OE of *HIF1A-AS1* inhibits metastasis of PC cells by transwell migration assay. (C) & (D) OE of *HIF1A-AS1* inhibits metastasis of PC cells by clone formation assays. (E) & (F) OE of *HIF1A-AS1* inhibits metastasis of PC cells by wound-healing assay. (n = 3 cultures, paired Student's t-test, ± SD) ** P<0.01, *** P<0.001

Figure 3. The summary of the iTRAQ-based proteomic analysis for *HIF-AS1* overexpression (OE) and normal control (NC) groups. (A) A shows the comparison of the CV values of different experimental groups more intuitively through the CV box diagram. The box diagrams of different colors represent the CV distribution of different experimental groups. The median CV of each box from left to right is 7.81% and 7.29%, respectively. (B) Distribution of the number of unique peptides obtained for all the proteins identified in this assay. (C) Peptide length distribution map of the identified peptides. (D) Sectors of different colors in the pie chart representing the percentage of protein with different ranges of identified coverage. (E) Statistical graph of different functions annotation results of. The abscissa indicates identification or different annotation methods, and the ordinate indicates the number of proteins corresponding to the abscissa. (F) GO analysis of the proportion of proteins involved in various biological processes.

Figure 4. Exploration of differentially expressed proteins (DEPs) and functional analysis. (A) Analyzing distribution of quantifiable multiples about difference proteins, the abscissa represents the value of multiples of difference after logarithmic transformation with base 2 as the base. The expression level greater than 0 shows up-regulated, and the expression level less than 0 shows down-regulated. (B) Volcano plot showing the distribution of proteins that are up-regulated (red) and down-regulated (blue) or showed no change (black) on overexpression of *HIF-AS*1. (C) Hierarchical clustering of proteins vs samples where rows represent the clustering of proteins, and columns represent the clustering of samples. As the protein abundance ratio changes from small to large, the heat map color shows a corresponding blue-white-red change. (D) KEGG analysis of the proportion of proteins involved in various biological processes.

Figure 5. Protein-protein interaction (PPI) network based on the differentially expressed proteins (DEPs). The total of 338 DEPs were filtered into the DEPs PPI network complex using the STRING online database. The round nodes indicate individual proteins.

Figure 6. The quantitative RT-PCR (qRT-PCR) validation of some differentially expressed proteins (DEPs) obtained from iTRAQ analysis in Overexpression (OE) of *HIF-AS1* and normal control (NC) groups. The expression levels of the same DEGs including *MX1*, *IFIH1*, *IFIT1*, *P4HB*, *ISG15* and *SOD2* were validated by RT-qPCR and normalized against *Actin* expression level. Values are normalized to those from cells with control vector. n=3, paired student's t test, ±SD. *P<0.1, **P<0.05, ***P<0.001. *MX1*, Interferon-induced GTP-binding protein Mx1; *IFIH1*, Interferon-induced helicase C domain-containing protein 1; *IFIT1*, Interferon-induced protein with tetratricopeptide repeats 1; *ISG15*, Ubiquitin-like protein ISG15; *P4HB*, Protein disulfide-isomerase; *SOD2*, Superoxide dismutase [Mn], mitochondrial.

Tables and Table Legends

Table 1. The genes and primers used for qRT-PCR experiments.

Gene	Forward primer (5'-3')	Reverse primer (5'-3')
MX1	GACAGGACCATCGGAATCTTGAC	GGGCTTCGGACAGGCTCAG
IFIH1	GGTGGTGATGATGAGTATTGTGATG	AGATTATTCCTCGTGCTGATTCCTC
IFIT1	GTGGACCCTGAAAACCCTGAATC	AGCGGACAGCCTGCCTTAG
P4HB	TGACGGCAAACTGAGCAACTTC	TCGGTGTGGTCGCTGTCG
ISG15	TGCTGGTGGTGGACAAATGC	CCCGCTCACTTGCTGCTTC
SOD2	GCACCACAGCAAGCACCAC	GATATGACCACCACCATTGAACTTC
Actin	TGGACTTCGAGCAAGAGATG	GAAGGAAGGCTGGAAGAGTG

Table 2. The all original data from the iTRAQ was analyzed using parameters.

These data were uploaded in Table 2.

Table 3. The 183 up-regulated DEPs were analyzed in OE VS NC.

These data were uploaded in Table 3.

Table 4. The 155 down-regulated DEPs were analyzed in OE VS NC.

These data were uploaded in Table 4.

Supplementary. The all original data included Table 2，Table 3 and Table 4.

These data were uploaded in Supplementary.

References

1. Kamisawa T, Wood LD, Itoi T, Takaori K: **Pancreatic cancer**. *Lancet* 2016, **388**(10039):73-85.
2. Torre LA, Bray F, Siegel RL, Ferlay J, Lortet-Tieulent J, Jemal A: **Global cancer statistics, 2012**. *CA Cancer J Clin* 2015, **65**(2):87-108.
3. Siegel RL, Miller KD, Jemal A: **Cancer statistics, 2018**. *CA Cancer J Clin* 2018, **68**(1):7-30.
4. Ferlay J, Soerjomataram I, Dikshit R, Eser S, Mathers C, Rebelo M, Parkin DM, Forman D, Bray F: **Cancer incidence and mortality worldwide: sources, methods and major patterns in GLOBOCAN 2012**. *Int J Cancer* 2015, **136**(5):E359-386.
5. Gzil A, Zarebska I, Bursiewicz W, Antosik P, Grzanka D, Szylberg L: **Markers of pancreatic cancer stem cells and their clinical and therapeutic implications**. *Mol Biol Rep* 2019, **46**(6):6629-6645.
6. Xu R, Yang J, Ren B, Wang H, Yang G, Chen Y, You L, Zhao Y: **Reprogramming of Amino Acid Metabolism in Pancreatic Cancer: Recent Advances and Therapeutic Strategies**. *Front Oncol* 2020, **10**:572722.
7. Huang X, Zhi X, Gao Y, Ta N, Jiang H, Zheng J: **LncRNAs in pancreatic cancer**. *Oncotarget* 2016, **7**(35):57379-57390.
8. Duguang L, Jin H, Xiaowei Q, Peng X, Xiaodong W, Zhennan L, Jianjun Q, Jie Y: **The involvement of lncRNAs in the development and progression of pancreatic cancer**. *Cancer Biol Ther* 2017, **18**(12):927-936.
9. Luo L, Wang M, Li X, Tian J, Zhang K, Tan S, Luo C: **Long non-coding RNA LOC285194 in cancer**. *Clin Chim Acta* 2020, **502**:1-8.
10. Guo W, Zhong K, Wei H, Nie C, Yuan Z: **Long non-coding RNA SPRY4-IT1 promotes cell proliferation and invasion by regulation of Cdc20 in pancreatic cancer cells**. *PLoS One* 2018, **13**(2):e0193483.
11. Ding M, Fu Y, Guo F, Chen H, Fu X, Tan W, Zhang H: **Long non-coding RNA MAFG-AS1 knockdown blocks malignant progression in breast cancer cells by inactivating JAK2/STAT3 signaling pathway via MAFG-AS1/miR-3196/TFAP2A axis**. *Int J Clin Exp Pathol* 2020, **13**(10):2455-2473.
12. Sanchez Calle A, Kawamura Y, Yamamoto Y, Takeshita F, Ochiya T: **Emerging roles of long non-coding RNA in cancer**. *Cancer Sci* 2018, **109**(7):2093-2100.
13. Tang Q, Hann SS: **HOTAIR: An Oncogenic Long Non-Coding RNA in Human Cancer**. *Cell Physiol Biochem* 2018, **47**(3):893-913.
14. Zhao X, Wang P, Liu J, Zheng J, Liu Y, Chen J, Xue Y: **Gas5 Exerts Tumor-suppressive Functions in Human Glioma Cells by Targeting miR-222**. *Mol Ther* 2015, **23**(12):1899-1911.
15. Chi Y, Wang D, Wang J, Yu W, Yang J: **Long Non-Coding RNA in the Pathogenesis of Cancers**. *Cells* 2019, **8**(9).
16. Qian CJ, Xu ZR, Chen LY, Wang YC, Yao J: **LncRNA MAFG-AS1 Accelerates Cell Migration, Invasion and Aerobic Glycolysis of Esophageal Squamous Cell Carcinoma Cells via miR-765/PDX1 Axis**. *Cancer Manag Res* 2020, **12**:6895-6908.
17. Yang G, Lu X, Yuan L: **LncRNA: a link between RNA and cancer**. *Biochim Biophys Acta* 2014, **1839**(11):1097-1109.
18. Xu J, Zhang Y, Chu L, Chen W, Du Y, Gu J: **Long non-coding RNA HIF1A-AS1 is upregulated in intracranial aneurysms and participates in the regulation of proliferation of vascular**

smooth muscle cells by upregulating TGF-beta1. *Exp Ther Med* 2019, **17**(3):1797-1801.

19. He Q, Tan J, Yu B, Shi W, Liang K: **Long noncoding RNA HIF1A-AS1A reduces apoptosis of vascular smooth muscle cells: implications for the pathogenesis of thoracoabdominal aorta aneurysm**. *Pharmazie* 2015, **70**(5):310-315.
20. Wang S, Zhang X, Yuan Y, Tan M, Zhang L, Xue X, Yan Y, Han L, Xu Z: **BRG1 expression is increased in thoracic aortic aneurysms and regulates proliferation and apoptosis of vascular smooth muscle cells through the long non-coding RNA HIF1A-AS1 in vitro**. *Eur J Cardiothorac Surg* 2015, **47**(3):439-446.
21. Wang J, Chen L, Li H, Yang J, Gong Z, Wang B, Zhao X: **Clopidogrel reduces apoptosis and promotes proliferation of human vascular endothelial cells induced by palmitic acid via suppression of the long non-coding RNA HIF1A-AS1 in vitro**. *Mol Cell Biochem* 2015, **404**(1-2):203-210.
22. Zhang QQ, Xu MY, Qu Y, Hu JJ, Li ZH, Zhang QD, Lu LG: **TET3 mediates the activation of human hepatic stellate cells via modulating the expression of long non-coding RNA HIF1A-AS1**. *Int J Clin Exp Pathol* 2014, **7**(11):7744-7751.
23. Wu Y, Ding J, Sun Q, Zhou K, Zhang W, Du Q, Xu T, Xu W: **Long noncoding RNA hypoxia-inducible factor 1 alpha-antisense RNA 1 promotes tumor necrosis factor-alpha-induced apoptosis through caspase 3 in Kupffer cells**. *Medicine (Baltimore)* 2018, **97**(4):e9483.
24. Zhang X, Li H, Guo X, Hu J, Li B: **Long Noncoding RNA Hypoxia-Inducible Factor-1 Alpha-Antisense RNA 1 Regulates Vascular Smooth Muscle Cells to Promote the Development of Thoracic Aortic Aneurysm by Modulating Apoptotic Protease-Activating Factor 1 and Targeting let-7g**. *J Surg Res* 2020, **255**:602-611.
25. Hong F, Gao Y, Li Y, Zheng L, Xu F, Li X: **Inhibition of HIF1A-AS1 promoted starvation-induced hepatocellular carcinoma cell apoptosis by reducing HIF-1alpha/mTOR-mediated autophagy**. *World J Surg Oncol* 2020, **18**(1):113.
26. Cribbs AP, Kennedy A, Gregory B, Brennan FM: **Simplified production and concentration of lentiviral vectors to achieve high transduction in primary human T cells**. *BMC Biotechnol* 2013, **13**:98.
27. Livak KJ, Schmittgen TD: **Analysis of relative gene expression data using real-time quantitative PCR and the 2(-Delta Delta C(T)) Method**. *Methods* 2001, **25**(4):402-408.
28. Ilic M, Ilic I: **Epidemiology of pancreatic cancer**. *World J Gastroenterol* 2016, **22**(44):9694-9705.
29. Zhou M, Ye Z, Gu Y, Tian B, Wu B, Li J: **Genomic analysis of drug resistant pancreatic cancer cell line by combining long non-coding RNA and mRNA expression profling**. *Int J Clin Exp Pathol* 2015, **8**(1):38-52.
30. Gong W, Tian M, Qiu H, Yang Z: **Elevated serum level of lncRNA-HIF1A-AS1 as a novel diagnostic predictor for worse prognosis in colorectal carcinoma**. *Cancer Biomark* 2017, **20**(4):417-424.
31. Tantai J, Hu D, Yang Y, Geng J: **Combined identification of long non-coding RNA XIST and HIF1A-AS1 in serum as an effective screening for non-small cell lung cancer**. *Int J Clin Exp Pathol* 2015, **8**(7):7887-7895.
32. Kim YS, Gupta Vallur P, Phaeton R, Mythreye K, Hempel N: **Insights into the Dichotomous Regulation of SOD2 in Cancer**. *Antioxidants (Basel)* 2017, **6**(4).
33. Miar A, Hevia D, Munoz-Cimadevilla H, Astudillo A, Velasco J, Sainz RM, Mayo JC: **Manganese**

superoxide dismutase (SOD2/MnSOD)/catalase and SOD2/GPx1 ratios as biomarkers for tumor progression and metastasis in prostate, colon, and lung cancer. *Free Radic Biol Med* 2015, **85**:45-55.

34. Brown SG, Knowell AE, Hunt A, Patel D, Bhosle S, Chaudhary J: **Interferon inducible antiviral MxA is inversely associated with prostate cancer and regulates cell cycle, invasion and Docetaxel induced apoptosis**. *Prostate* 2015, **75**(3):266-279.
35. Andersson I, Bladh L, Mousavi-Jazi M, Magnusson KE, Lundkvist A, Haller O, Mirazimi A: **Human MxA protein inhibits the replication of Crimean-Congo hemorrhagic fever virus**. *J Virol* 2004, **78**(8):4323-4329.
36. Imaizumi T, Satake U, Miyashita R, Kawaguchi S, Matsumiya T, Seya K, Ding J, Tanaka H: **Interferon-induced transmembrane protein 1 and Myxovirus resistance protein 1 are induced by polyinosinic-polycytidylic acid in cultured hCMEC/D3 human cerebral microvascular endothelial cells**. *J Neuroimmunol* 2019, **337**:577047.
37. Abbas YM, Pichlmair A, Gorna MW, Superti-Furga G, Nagar B: **Structural basis for viral 5'-PPP-RNA recognition by human IFIT proteins**. *Nature* 2013, **494**(7435):60-64.
38. Pidugu VK, Wu MM, Yen AH, Pidugu HB, Chang KW, Liu CJ, Lee TC: **IFIT1 and IFIT3 promote oral squamous cell carcinoma metastasis and contribute to the anti-tumor effect of gefitinib via enhancing p-EGFR recycling**. *Oncogene* 2019, **38**(17):3232-3247.
39. Pidugu VK, Pidugu HB, Wu MM, Liu CJ, Lee TC: **Emerging Functions of Human IFIT Proteins in Cancer**. *Front Mol Biosci* 2019, **6**:148.
40. Jiang M, Osterlund P, Sarin LP, Poranen MM, Bamford DH, Guo D, Julkunen I: **Innate immune responses in human monocyte-derived dendritic cells are highly dependent on the size and the 5' phosphorylation of RNA molecules**. *J Immunol* 2011, **187**(4):1713-1721.
41. Zhang J, Liu X, Meng Y, Wu H, Wu Y, Yang B, Wang L: **Autoimmune disease associated IFIH1 single nucleotide polymorphism related with IL-18 serum levels in Chinese systemic lupus erythematosus patients**. *Sci Rep* 2018, **8**(1):9442.
42. Zhao C, Denison C, Huibregtse JM, Gygi S, Krug RM: **Human ISG15 conjugation targets both IFN-induced and constitutively expressed proteins functioning in diverse cellular pathways**. *Proc Natl Acad Sci U S A* 2005, **102**(29):10200-10205.
43. Hsiang TY, Zhao C, Krug RM: **Interferon-induced ISG15 conjugation inhibits influenza A virus gene expression and replication in human cells**. *J Virol* 2009, **83**(12):5971-5977.

Figures

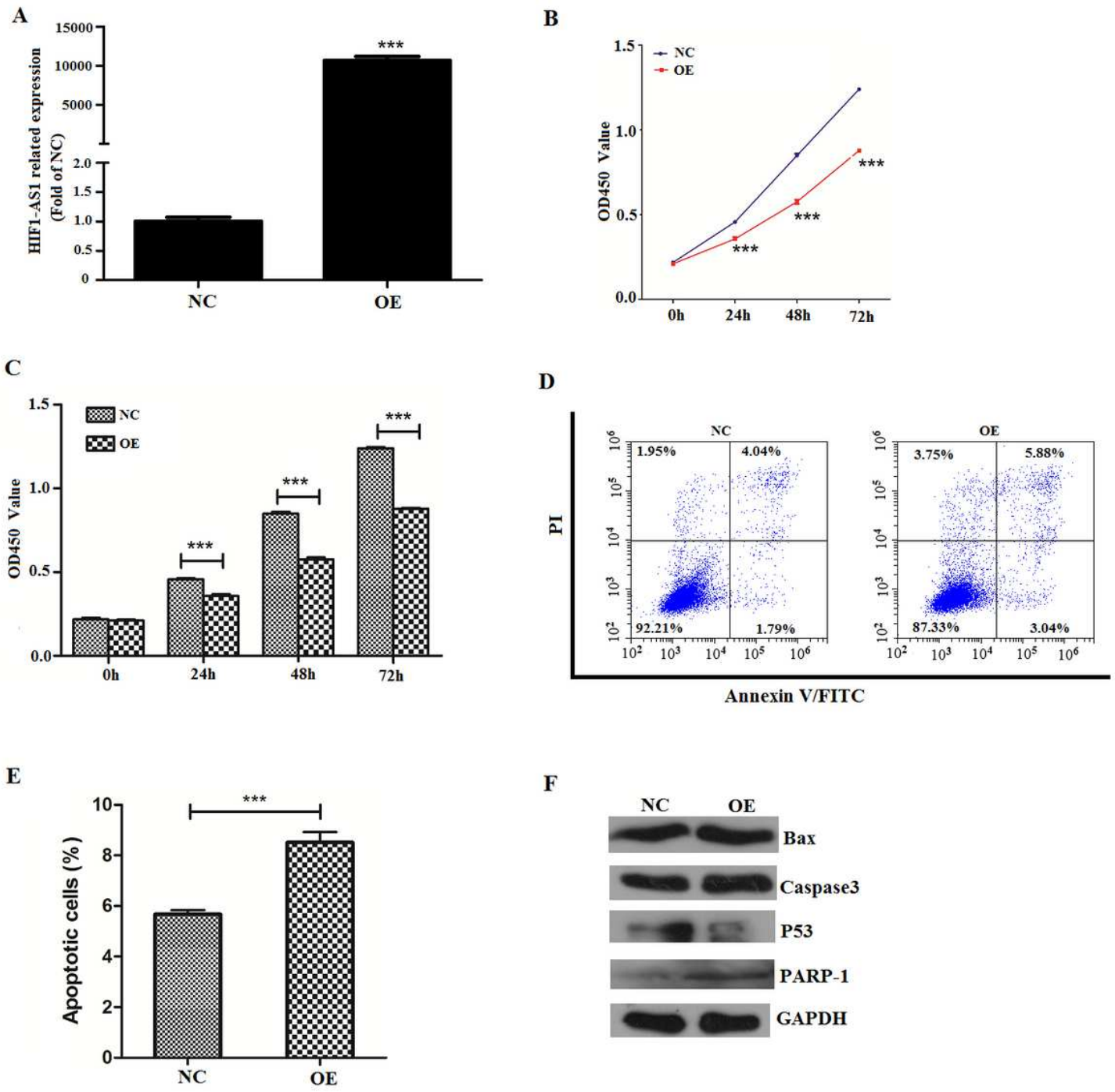

Figure 1

Overexpression (OE) of HIFA-AS1 affects the proliferation, apoptosis of the pancreatic cancer (PC) cells (Pan-1). (A) Real time PCR showed that the levels of HIF1A AS1 was significantly incre a sed in the cells from OE group compared with normal control (NC) NC). (B) & C) OE of HIF1A AS1 reduces significantly the viability of PC cells at 24, 48, and 72 h. (D) OE of HIF1A AS1 promotes significantly apoptosis of PC cells assessment of cellular apoptosis using Annexin V fluorescein isothiocyanate staining coupled with flow cytometry. (Total percentage of apoptotic PANC 1 cells in each group are summarized with data

presented as the mean ± SD of three independent experiments. (F) Western blotting reveal Cleaved caspase-3, Bax, P53, and PARP-1A protein expression in PANC 1 cells. ***P<0.001

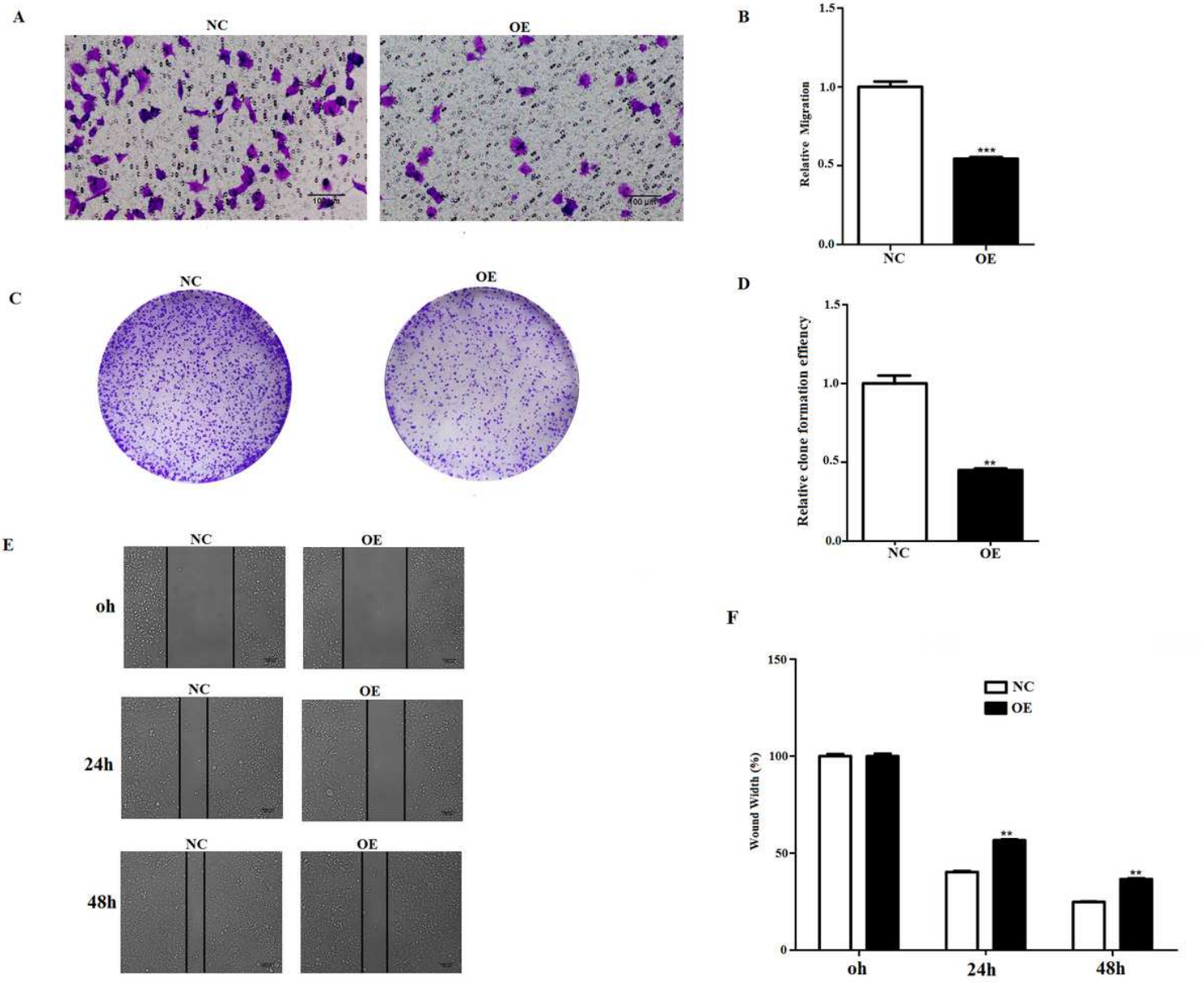

Figure 2

Overexpression (OE) of HIF1A-AS1 regulates metastasis of the pancreatic cancer (PC) cells (Pan-1). (A) & (B) OE of HIF1A AS1 inhibits metastasis of PC cells by transwell migration assay. (C) & (D) OE of HIF1A AS1 inhibits metastasis of PC cells by clone formation assays. (E) & (F) OE of HIF1A AS1 inhibits metastasis of PC cells by wound healing assay. (n = 3 cultures, paired Student's t test, ± ** P<0.01, *** P<0.001

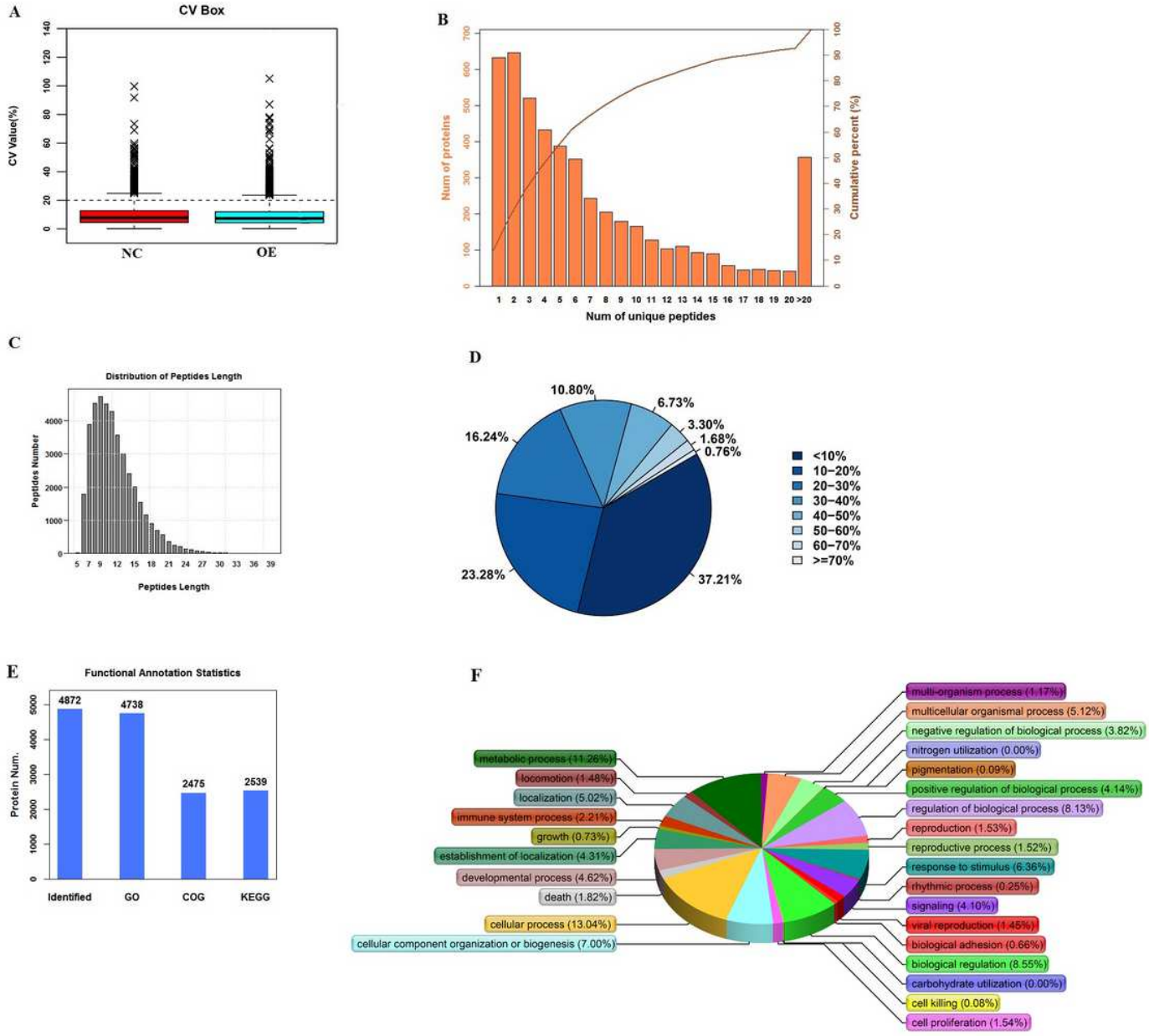

Figure 3

The summary of the iTRAQ-based proteomic analysis for HIF-AS1 overexpression (OE) and normal control (NC) groups. (A) A shows the comparison of the CV values of different experimental groups more intuitively through the CV box diagram. The box diagrams of different colors represent the CV distribution of different experimental groups. The median CV of each box from left to right is 7.81% and 7.29%, respectively. (B) Distribution of the number of unique peptides obtained for all the proteins identified in this assay. (C) Peptide length distribution map of the identified peptides. (D) Sectors of different colors in the p ie chart representing the percentage of protein with different ranges of identified coverage coverage. (E) Statistical graph of different functions annotation results of. The abscissa indicates identification or different annotation methods, and the ordinate indica tes the number of proteins corresponding to the abscissa. (F) GO analysis of the proportion of proteins involved in various biological processes.

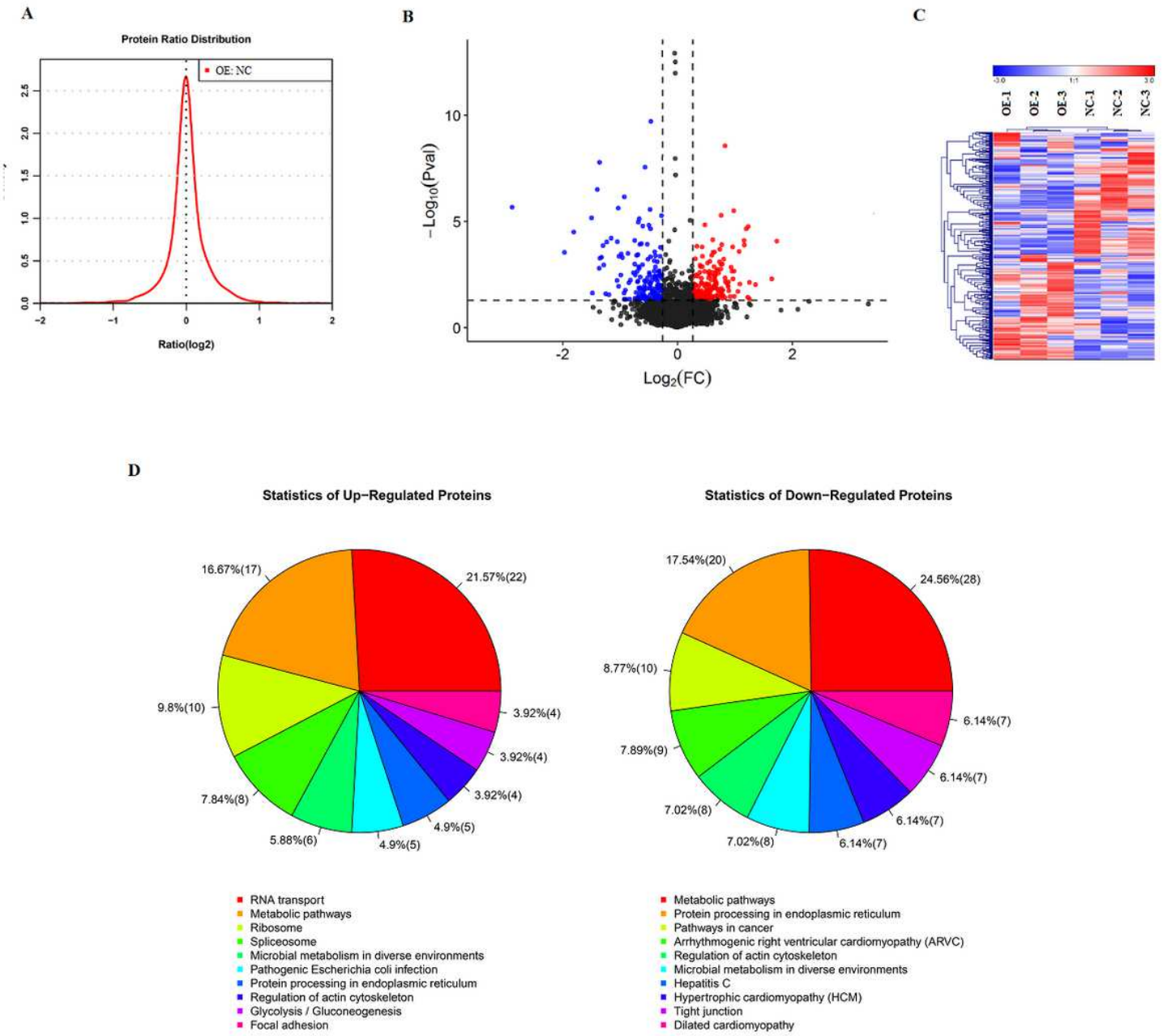

Figure 4

Exploration of differentially expressed proteins (DEPs) and functional analysis. (A) Analyzing distribution of quantifiable multiples about difference proteins, the abscissa represents the value of multiples of difference after logarithmic transformation with base 2 as the base. The expression level greater than 0 shows up-regulated, and the expression level less than 0 shows down-regulated. (B) Volcano plot showing the distribution of proteins that are up regulated (red) and down regulated (blue) or showed no change (black) on overexpression of HIF AS 1. (C) Hierarchical clustering of prote ins vs samples where rows represent the clustering of proteins, and columns represent the clustering of samples. As the protein abundance ratio changes from small to large, the heat map color shows a corresponding blue white red change. (D) KEGG analysis of the proportion of proteins involved in various biological processes.

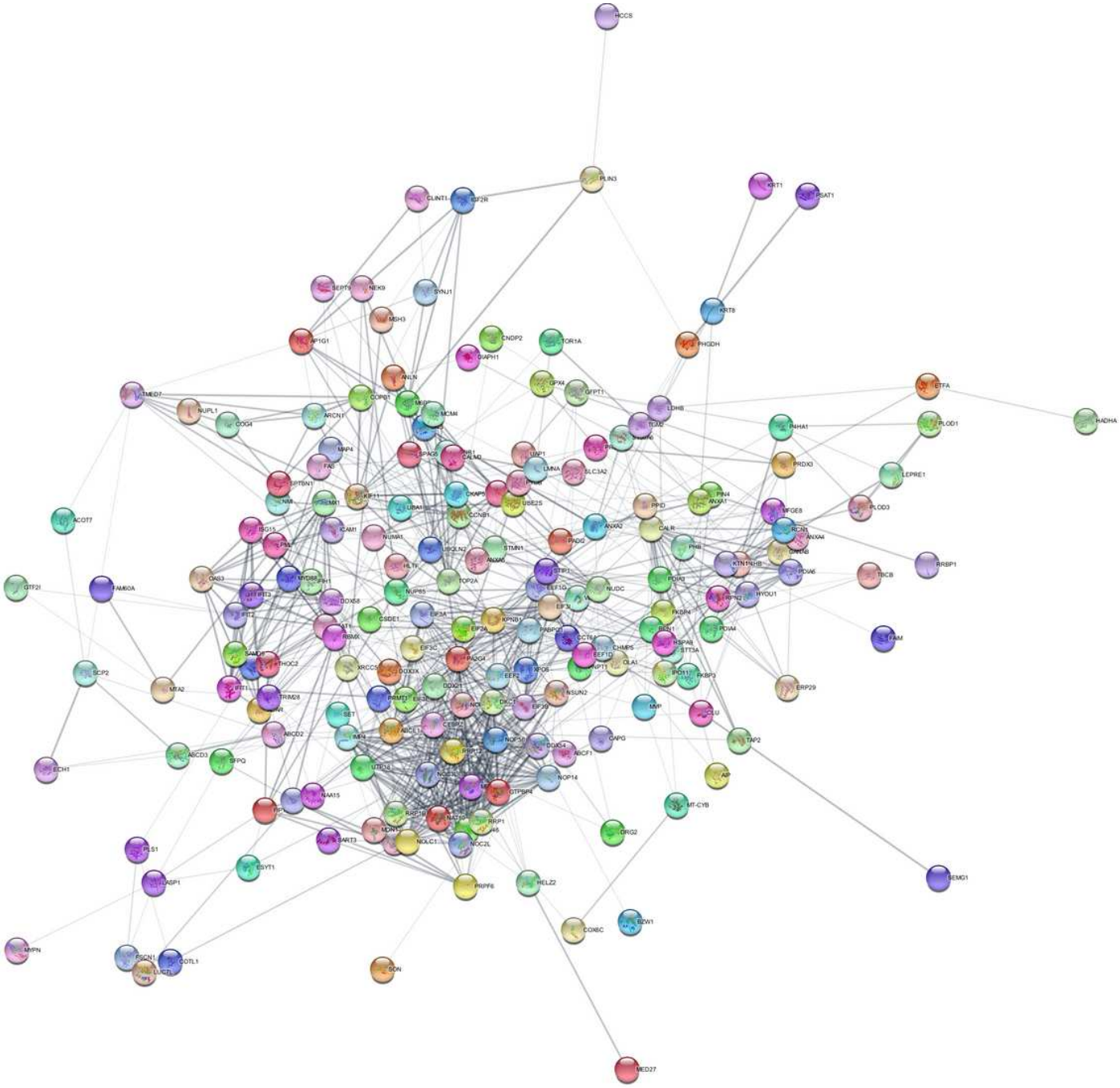

Figure 5

Protein-protein interaction (PPI) network based on the differentially expressed proteins (DEPs). The total of 338 DEPs were filtered into the DEPs PPI network complex using the STRING online database. The round nodes indicate individual proteins.

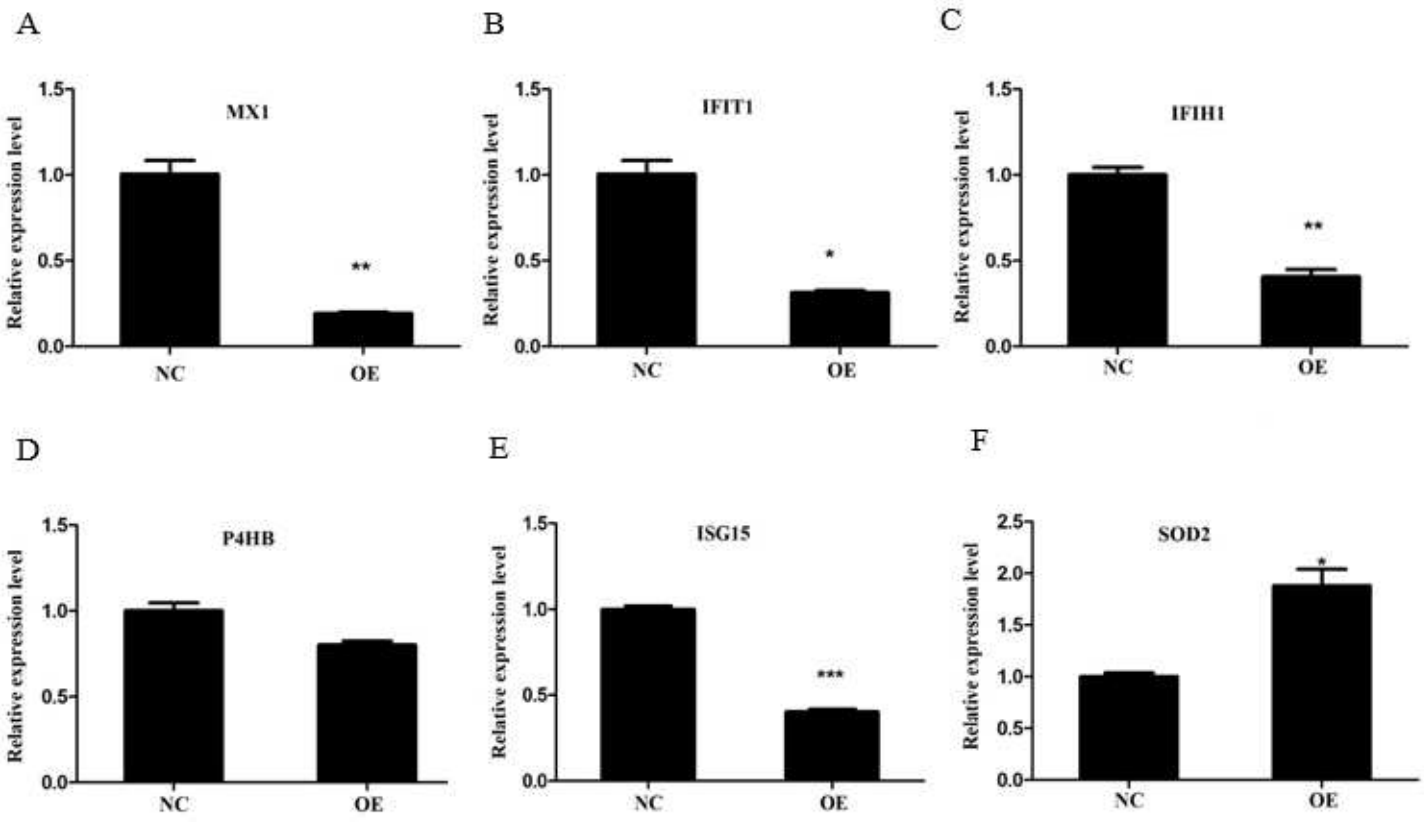

Figure 6

The quantitative RT-PCR (qRT-PCR) validation of some differentially expressed proteins (DEPs) obtained from iTRAQ analysis in Overexpression (OE) of HIF-AS1 and normal control (NC) groups. The expression levels of the same DEGs including MX1 IFIH1 IFIT1 P4HB ISG15 and SOD2 were validated by RT □ qPCR and normalized against Actin expression level. Values are normalized to those from cells with control vector. n=3, paired student's t test, ±SD. *P<0.1, **P<0.05, ***P< MX1 , Interferon induced GTP binding protein Mx1; IFIH1 , Interferon induced helicase C domain containing protein 1; IFIT1 , Interferon induced protein with tetratricopeptid e repeats 1; ISG15 , Ubiquitin like protein ISG15; P4HB , Protein disulfide isomerase; SOD2 , Superoxide dismutase [Mn],mitochondrial.

Supplementary Files

This is a list of supplementary files associated with this preprint. Click to download.

- Table2.xlsx
- Table3.xlsx
- Table4.xlsx
- supplementary.xlsx